

Synthesis and biological evaluation of farnesylthiosalicylamides as potential anti-tumor agents



Yong Ling^{a,b}, Zhiqiang Wang^{a,b}, Hongyan Zhu^b, Xuemin Wang^b, Wei Zhang^b, Xinyang Wang^b, Li Chen^a, Zhangjian Huang^{a,c,*}, Yihua Zhang^{a,c,*}

^aState Key Laboratory of Natural Medicines, China Pharmaceutical University, Nanjing 210009, PR China

^bMedical College, Nantong University, Nantong 226001, PR China

^cCenter of Drug Discovery, China Pharmaceutical University, Nanjing 210009, PR China

ARTICLE INFO

Article history:

Received 17 August 2013

Revised 17 October 2013

Accepted 8 November 2013

Available online 15 November 2013

Keywords:

Farnesylthiosalicylic acid

Diamines

Cell apoptosis

Ras-related signaling pathway

Anti-cancer agents

ABSTRACT

Fourteen hybrids of farnesylthiosalicylic acid (FTS) with various diamines were synthesized and biologically evaluated. It was found that FTS-monoamide molecules (**10a–g**) displayed strong anti-proliferative activity against seven human cancer cell lines, superior to FTS and FTS-bisamide compounds (**11a–g**). The mono-amide **10f** was the most active, with IC₅₀s of 3.78–7.63 μM against all tested cancer cells, even more potent than sorafenib (9.12–22.9 μM). In addition, **10f** induced SMMC-7721 cell apoptosis, down-regulated the expression of Bcl-2 and up-regulated Bax and caspase-3. Furthermore, **10f** had the improved aqueous solubility relative to FTS. Finally, treatment with **10f** dose-dependently inhibited the Ras-related signaling pathways in SMMC-7721 cells. Collectively, **10f** could be a promising candidate for the intervention of human cancers.

© 2013 Elsevier Ltd. All rights reserved.

1. Introduction

The Ras proteins are low molecular-weight GTP-binding proteins, which function as biological switches playing a key role in mediation of signal transduction between G-protein-coupled receptors and downstream events, such as mitogen-activated protein kinase (MAPK) and Akt.^{1,2} Mutations or excessive activation of Ras proteins are found in approximately 30% of human cancers.^{3–5} It was reported that the inhibition of excessive activated Ras proteins may revert malignant cells to a nonmalignant phenotype and cause tumor regression both in vitro and in vivo.⁶ As a result, the Ras protein has become an attractive therapeutic target for intervention of a number of cancers.

Farnesylthiosalicylic acid (FTS, Fig. 1), structurally mimicking the carboxyl-terminal farnesylcysteine moiety of Ras proteins, can recognize the anchorage and dislodge the active Ras protein from the cell membrane, thereby blocking the initiation of downstream signaling events, inhibiting tumor cell proliferation and promoting the tumor cell apoptosis.^{7–9} Although FTS was well preclinically studied for the treatment of a wide range of malignancies, including lung, breast, and pancreatic cancers,^{10–13} it has not got approval for clinical trials mainly due to its limited therapeutic efficacy.¹⁴ Therefore, development of new FTS-based Ras inhibitors

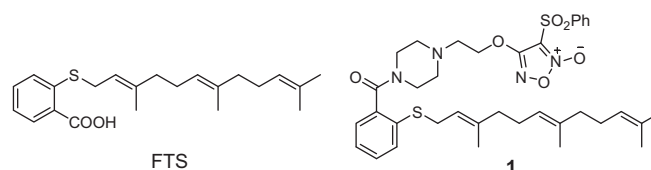


Figure 1. The chemical structures of FTS and furoxan-based nitric oxide derivative of FTS (compound **1**).

with more potent anti-tumor activity should be of clinical significance.

Previously, a series of furoxan-based nitric oxide donating FTS derivatives with anti-hepatocellular carcinoma activity was reported by our group.¹⁵ It has been observed that the amide derivatives exhibit much stronger inhibitory effects than the corresponding esters. The most active compound **1** is an amide bearing a piperazine moiety (Fig. 1). It is known that a diamine moiety exists in various pharmaceutical compounds¹⁶ and is often used as a structural block in rational drug design because of its improved water-solubility and enhanced bioavailability and metabolic stability in vivo.¹⁷ It was therefore interesting to determine whether conjugating such diamine moiety with the carboxylic acid group of FTS would provide the derivatives that possess enhanced anticancer activity as well as the desired water-solubility. As part of this ongoing program, we now describe the synthesis of

* Corresponding authors. Tel./fax: +86 2583271015 (Y.Z.).

E-mail addresses: zyhtgd@hotmail.com, zyhtgd@163.com (Y. Zhang).

mono- (**10a–g**) and bis-amides (**11a–g**) of FTS, and evaluation as potential anti-cancer agents.

2. Results and discussion

2.1. Chemistry

FTS was previously prepared by direct conjugation of thiosalicylic acid with farnesyl bromide in the presence of guanidine carbonate,¹⁸ but some disadvantages limit the utility of this approach. Firstly, hydrogen-bonding effect between the carboxyl with the sulfhydryl of thiosalicylic acid could attenuate the reactivity of sulfhydryl with farnesyl bromide. Secondly, the carboxyl of thiosalicylic acid could also react with farnesyl bromide, producing some by-products, reducing the yields and leading to purification problem. Herein, FTS was obtained using a protection strategy. The synthetic routes of **10a–g** and **11a–g** including FTS are depicted in Scheme 1. Triethylphosphonoacetate (TEPA) was treated with (*E*)-geranyl acetone (**2**) in the presence of NaH to form (*E,E*)-ethyl farnesylate (**3**) as previously reported.¹⁹ Compound **3** was reduced by LiAlH₄ giving (*E,E*)-farnesol (**4**), which was then converted to (*E,E*)-farnesyl bromide (**5**) by treatment with PBr₃. In addition, the carboxyl group of thiosalicylic acid (**6**) was protected to form methyl thiosalicylate (**7**). Coupling of **5** with **7** furnished methyl (*E,E*)-farnesylthiosalicylate (FTM, **8**), followed by hydrolysis in aqueous solution of NaOH to provide free carboxylic acid (FTS, **9**). Subsequently, **9** was treated with oxalylchloride to produce (*E,E*)-farnesylthiosalicyl chloride, which was treated without further purification with several diamines including cyclic piperazine in the presence of triethylamine, giving target compounds **10a–g** and **11a–g**. The target compounds **10a–g** and **11a–g** were purified by column chromatography, and their structures were characterized by IR, ¹H NMR and MS.

2.2. Biological evaluation

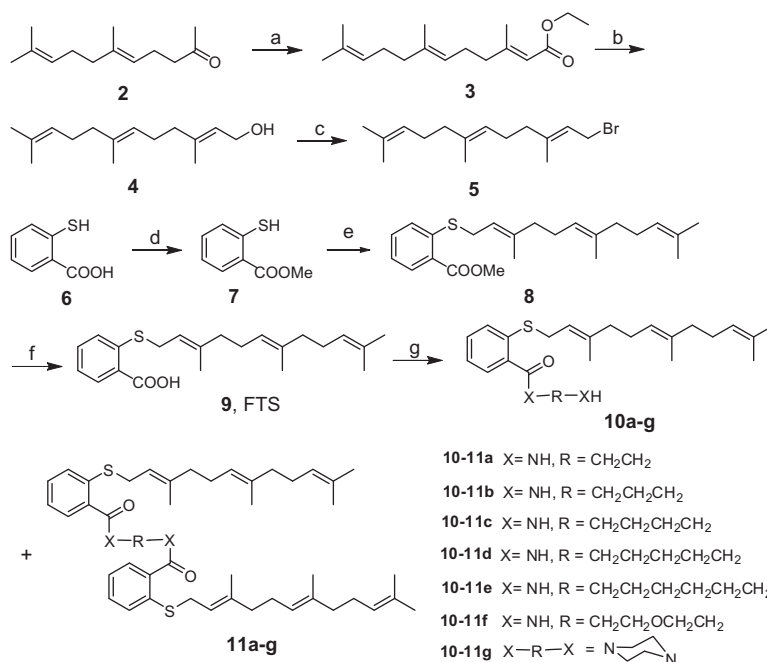
The cell growth inhibitory activity of target compounds **10a–g** and **11a–g** against seven human cancer cell lines SGC7901 (human

gastric cancer cells), SMMC-7721 (human hepatocellular carcinoma cells), EJ (human bladder carcinoma cells), SKOV-3 (human ovarian cancer cells), MCF-7 (human breast cancer cells), H460 (human lung cancer cells), Panc-1 (human pancreatic carcinoma cells) were evaluated by MTT assays *in vitro* using FTS and sorafenib, a well-known Ras-related signal inhibitor, as positive controls. The IC₅₀ values were summarized in Table 1. As can be seen, mono-amides **10a–g** displayed dramatically improved antiproliferative effects compared to FTS. Among them, compounds **10c–f** (IC₅₀ = 3.78–15.0 μM) showed slightly stronger antiproliferative effects than sorafenib (IC₅₀ = 9.12–22.9 μM). Notably, **10f** exhibited most potent inhibitory activity with IC₅₀ value range of 3.78–7.63 μM against all tested cancer cells. However, compounds **11a–f**, the bis-amide derivatives of FTS showed very weak inhibitory activity.

Given that FTS is a known Ras inhibitor and could block Ras-related signaling events, inducing tumor cell apoptosis, the most active compound **10f** was selected to determine its effect on SMMC-7721 cells apoptosis. The SMMC-7721 cells were incubated with vehicle alone or with different concentrations of **10f** (3, 6 or 12 μmol/L), or FTS (12 μmol/L) for 48 h, and the percentages of the apoptotic SMMC-7721 cells were determined by FITC-Annexin V/PI staining and flow cytometry. As shown in Figure 2, the percentage of annexin V + apoptotic SMMC-7721 cells gradually increased for those cells exposed to increasing concentrations of **10f** (25.9% for 3 μmol/L; 48.2% for 6 μmol/L; and 84.5% for 12 μmol/L), demonstrating that incubation with **10f** induced SMMC-7721 cell apoptosis in a dose-dependent manner. In contrast, incubations performed using FTS (12 μmol/L) only induced apoptosis of 19.4% SMMC-7721 cells.

Next, a Western blotting analysis was conducted to check the expression levels of Bcl-2, Bax and caspase-3 proteins. It was observed that incubation of **10f** significantly increased levels of pro-apoptotic Bax and caspase 3, but reduced levels of anti-apoptotic Bcl-2 (Fig. 3) in a dose-dependent manner.

Finally, in order to get insight to the mechanisms underlying the activity of these farnesylthiosalicylamide derivatives, we examined the inhibitory effects of the active compound **10f** on the Ras-re-



Scheme 1. Reaction reagents and conditions: (a) TEPA, NaH, ether, 0 °C to rt, 12 h, 81%; (b) LiAlH₄, AlCl₃, ether, 0 °C to rt, 4 h, 88%; (c) PBr₃, pyridine, *n*-hexane, ether, 0 °C to rt, 4 h, 76%; (d) SOCl₂, MeOH, 0 °C-reflux, 8 h, 85%; (e) **5**, K₂CO₃, CH₃CN, 50 °C, 6 h; (f) 1 N NaOH, MeOH, 60 °C, 10 h, 82%; (g) oxalylchloride, diamines or piperazine, TEA, CH₂Cl₂, 0 °C to rt, 2 h.

Table 1
The IC₅₀ values of **10a–g** and **11a–g** against seven human cancer cell lines

Compd	In vitro inhibition of human cancer cells proliferation (IC ₅₀ ^a , μM)						
	SGC-7901	SMMC-7721	EJ	SKOV-3	MCF-7	H460	Panc-1
FTS	41.3 ± 5.56	69.7 ± 3.85	47.6 ± 3.28	51.2 ± 5.06	49.1 ± 4.66	49.2 ± 4.47	53.6 ± 5.77
Sorafenib	11.5 ± 2.71	18.7 ± 2.65	22.9 ± 3.53	9.25 ± 2.15	9.12 ± 1.80	10.8 ± 2.36	12.3 ± 1.46
10a	33.8 ± 3.68	25.2 ± 3.59	>50	31.6 ± 2.81	28.7 ± 3.42	36.0 ± 3.83	>50
10b	12.8 ± 1.76	10.6 ± 1.84	17.2 ± 1.37	12.3 ± 1.92	13.7 ± 2.01	20.4 ± 3.36	11.8 ± 1.25
10c	11.2 ± 0.97	15.0 ± 1.67	13.1 ± 1.49	7.80 ± 1.01	11.2 ± 1.33	12.5 ± 1.62	10.5 ± 1.38
10d	7.35 ± 0.88	9.21 ± 1.13	9.85 ± 1.24	7.13 ± 0.94	7.83 ± 0.68	8.84 ± 1.10	7.56 ± 1.17
10e	7.87 ± 1.06	7.93 ± 1.20	10.1 ± 0.77	7.66 ± 1.05	8.01 ± 0.93	7.52 ± 0.89	8.69 ± 1.09
10f	7.63 ± 0.90	5.71 ± 0.69	6.13 ± 0.52	6.83 ± 0.71	7.29 ± 0.93	6.89 ± 0.85	3.78 ± 0.45
10g	25.7 ± 2.75	32.4 ± 2.94	27.5 ± 3.67	>50	34.1 ± 3.01	26.3 ± 2.64	22.5 ± 2.96
11a	>50	>50	>50	>50	>50	>50	>50
11b	>50	>50	>50	>50	>50	>50	>50
11c	>50	>50	>50	>50	45.8 ± 3.99	>50	>50
11d	>50	36.2 ± 3.75	39.5 ± 4.18	41.9 ± 3.54	>50	47.1 ± 3.26	>50
11e	>50	>50	43.9 ± 4.71	>50	40.6 ± 3.66	>50	>50
11f	43.8 ± 5.25	29.0 ± 3.32	27.8 ± 3.07	34.4 ± 4.28	30.0 ± 3.62	43.5 ± 3.27	29.8 ± 3.03
11g	>50	>50	>50	>50	>50	>50	>50

^a The inhibitory effects of individual compounds on the proliferation of cancer cell lines were determined by the MTT assay. The data are the mean values of IC₅₀ (a dose achieved 50% inhibition in the proliferation of cancer cells cultured) ± SEM from at least three independent experiments.

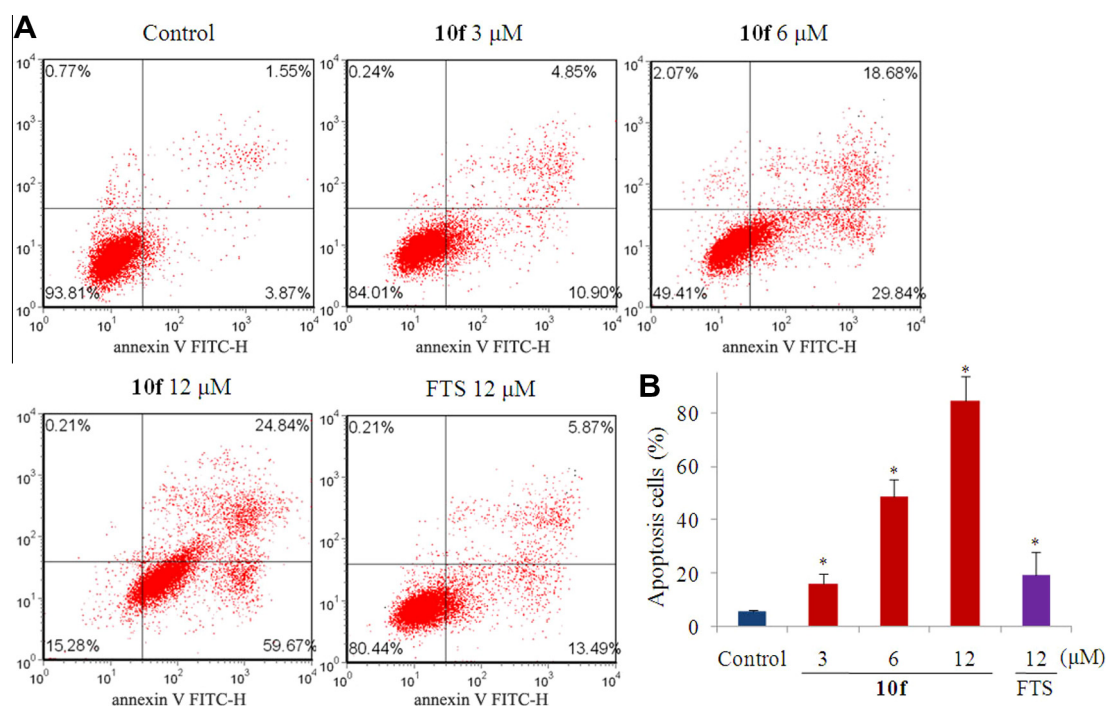


Figure 2. Compound **10f** induced SMMC-7721 cell apoptosis in vitro. SMMC-7721 cells were incubated with the indicated concentrations of **10f** and 12 μM FTS for 48 h, and the cells were stained with FITC-Annexin V and PI, followed by flow cytometry analysis. (A) Flow cytometry analysis. (B) Quantitative analysis of apoptotic cells. Data are expressed as means ± SEM of the percentages of apoptotic cells from three independent experiments. **P* < 0.01 versus control.

lated signaling in SMMC-7721 cells using FTS as control. The cells were incubated with vehicle alone, FTS (12 μM), or with **10f** (3, 6 or 12 μM). The expression and phosphorylation levels of the Ras-related signal events, Akt, and ERK1/2 (extracellular signal-regulated kinase 1/2) were determined using an immunoblotting assays. As shown in Figure 4, after the treatment with **10f**, the levels of phospho-ERK1/2 and phospho-Akt were clearly reduced in SMMC-7721 cells in a dose-dependent manner, and at the same concentration of 12 μM, treatment with **10f** showed the lower levels relative to FTS. Meanwhile the similar expression levels of ERK and Akt were observed in groups treated with **12f** and FTS, respectively. The results demonstrated that the inhibition of Ras-related signaling pathways by **10f** may contribute to its significant antitumor

activities in the growth inhibition and apoptosis induction of the cancer cell lines.

2.3. Aqueous solubility determination

The aqueous solubility of parent compound FTS, some selected FTS mono-amide (**10d**, **10f**) and bis-amide (**11d**) derivatives in 10% PEG400 aqueous solution was determined using a previously reported HPLC-based method.²⁰ As shown in Table 2, the solubility of mono-amides **10d**, **10f** were 17.97 and 23.75 mg/mL, respectively, which were six to eightfold better than that of FTS (3.65 mg/mL). Obviously, compound **10f** with an oxygen atom displaced in the diamine chain of **10d**, got an improved solubility.

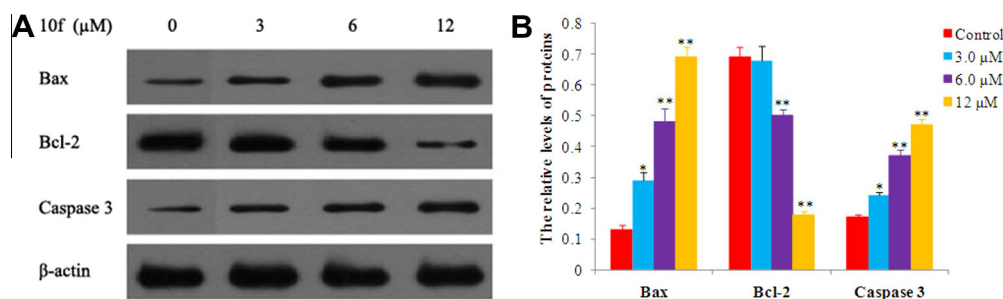


Figure 3. Effect of **10f** on the expression of apoptosis-related proteins in SMMC-7721 cells. (A) The expression of Bax, Bcl2, caspase 3 and β -actin was examined by Western blot analysis. SMMC-7721 cells were incubated with, or without, **10f** at the indicated concentrations for 48 h and the levels of protein expression were detected using specific antibodies, and β -actin was used as the control. Data shown are representative images of each protein for three separate experiments. (B) Quantitative analysis: the relative levels of each protein compared to control β -actin were determined by densitometric scanning. Data are expressed as means \pm SEM from three separate experiments. * P <0.05 versus control; ** P <0.01 versus control.

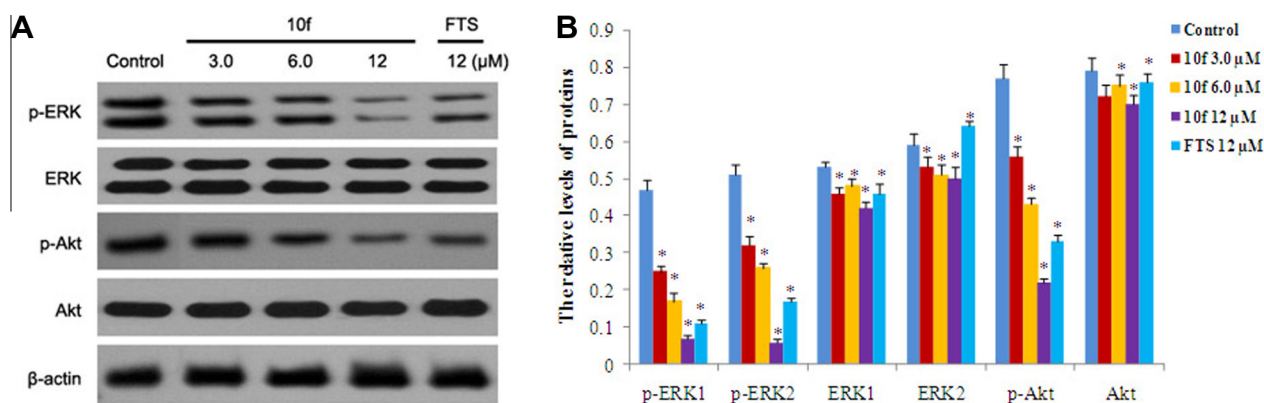


Figure 4. Immunoblot analysis of the expression and phosphorylation of Akt and ERK1/2 in vitro. (A) SMMC-7721 cells were treated with vehicle (control), FTS, or different doses of **10f** were homogenized, and their lysates were subjected to immunoblot analysis using anti-ERK1/2, antiphospho-ERK1/2 (Thr202/Tyr204), anti-Akt, antiphospho-Akt (Ser473), and anti- β -actin antibodies, respectively. β -Actin was used as the control. (B) Quantitative analysis. The relative levels of each signaling event to control β -actin were determined by densitometric scanning. The data are expressed as means \pm SEM of three duplicate experiments. * P <0.01 versus control.

Table 2
Solubilities and log P values of the selected compounds in PEG400 aqueous solution

Compound	Solubility (mg/mL)	Log P
FTS	3.65	6.32
10d	17.97	5.98
10f	23.75	4.85
11d	<0.01	14.04

In contrast, the solubility of bis-amide derivative **11d** was less than 0.01 mg/mL. The log P values of these compounds were also calculated by ChemBioDraw Ultra (version 2008). It was found that the log P values of mono-amides **10d** and **10f** were lower than that of FTS, and compound **11d** had the highest log P value of 14.04.

2.4. Structure–activity relationships (SARs) analysis

Analysis of SAR revealed that FTS-monoamides **10a–g** displayed stronger anti-proliferative activity than bis-amides derivatives **11a–g** against seven tested cancer cells. It is likely that monoamide derivatives with a free amine moiety possess better aqueous solubility and suitable log P values, which could be beneficial for them to penetrate the cancer cells and bind more effectively to the galectin site of Ras protein, blocking Ras-related signaling events. Among the monoamides, compounds **10d–f** bearing five or six-atom length of diamines moiety exerted the most potent effects against tumor cells growth. In addition, substitution of one oxygen atom for methylene in the diamine chain of **10d** leading

to **10f** could further improve the solubility, thus enhancing the biological activity.

3. Conclusions

In summary, a series of hybrids of FTS with various diamines were synthesized, and their anti-proliferative activity and aqueous solubility were evaluated. The FTS mono-amides with better aqueous solubility displayed stronger inhibitory activity than FTS and bis-amides derivatives **11a–g**. The mono-amide **10f** was the most active, with IC₅₀s of 3.78–7.63 μ M against all tested cancer cells, even more potent than sorafenib, a well-known anti-cancer drug. Additionally, **10f** could induce tumor cell apoptosis, reduce the protein levels of Bcl-2, and increase the expression of Bax and caspase-3 proteins. More importantly, treatment with **10f** inhibited the Ras-related signaling pathways in a dose-dependent manner in the cancer cells. Our findings suggest that diamine-based FTS modification could be a useful way to enhance the anti-cancer activity of FTS. Further studies on **10f** are warranted for the treatment of human cancers.

4. Experimental section

4.1. Chemistry

Infrared (IR) spectra (KBr) were recorded on a Nicolet Impact 410 instrument (KBr pellet). ¹H NMR spectra were recorded with a BrukerAvance 300 MHz spectrometer at 300 K, using TMS as an

internal standard. MS spectra were recorded on a Mariner Mass Spectrum (ESI). Element analysis was performed on an Eager 300 instrument. All compounds were routinely checked by TLC and ^1H NMR. TLCs and preparative thin-layer chromatography were performed on silica gel GF/UV 254, and the chromatograms were conducted on silica gel (200–300 mesh, Merck) and visualized under UV light at 254 and 365 nm. All solvents were reagent grade and, when necessary, were purified and dried by standard methods. Compounds **2** and **6** were commercially available. Solutions after reactions and extractions were concentrated using a rotary evaporator operating at a reduced pressure of ca. 20 Torr.

4.1.1. (2E,6E)-Ethyl 3,7,11-trimethyldodeca-2,6,10-trienoate (3)

To a solution of NaH (60%, 3.20 g, 80 mmol) in anhydrous THF (200 mL), triethylphosphonoacetate (TEPA) (9.00 g, 40 mmol) in anhydrous THF (50 mL) was added dropwise at 0 °C according to the literature.¹⁹ The obtained mixture was stirred for 2 h at the room temperature and then was cooled to 0 °C again. Then (*E*)-geranyl acetone (**2**) (4.90 g, 25 mmol) was added dropwise, and the mixture was allowed to rise to the room temperature and stir for 4 h. The reaction mixture was poured into water (250 mL), and extracted with diethyl ether (300 mL \times 3). The combined organic layer was washed with water and brine, dried over anhydrous Na_2SO_4 , and concentrated in vacuo. The residue was purified by silica chromatography (petroleum ether/ethyl acetate = 40:1, v/v as the eluent), affording the *E,E* product **3** 4.20 g and *Z,E* isomers (*Z,Z*,*6E*)-ethyl 3,7,11-trimethyldodeca-2,6,10-trienoate 1.15 g, colorless liquid, total yield 81%.¹⁹

4.1.2. (2E,6E)-3,7,11-Trimethyldodeca-2,6,10-trien-1-ol (4)

To a solution of LiAlH_4 (1.20 g, 31 mmol) in anhydrous diethyl ether (100 mL) was added AlCl_3 (1.47 g, 11 mmol), then compound **3** (4.20 g, 17 mmol) in diethyl ether was slowly added at –5 °C. The mixture was stirred for 1 h, and then hydrolyzed with 2 N NaOH until the formation of white granule. The precipitation was removed by filtration and the filtrate was extracted with ethyl ether (100 mL \times 3). The combined organic layers were dried with anhydrous Na_2SO_4 and concentrated in vacuo. The crude product was purified by silica chromatography (petroleum ether–ethyl acetate = 4:1, v/v as the eluent), affording compound **4** as a colorless liquid (3.11 g, 88%). ^1H NMR (CDCl_3 , 300 MHz, δ ppm): 5.33 (bt, 1H, SCH_2CH), 5.09 (bt, 2H, $2 \times \text{CH}_2\text{CH}=\text{CCH}_3$), 4.12–4.15 (m, 2H, OCH_2), 1.90–2.02 (m, 8H, $2 \times \text{CCH}_2\text{CH}_2\text{CH}$), 1.54–1.68 (m, 12H, $4 \times \text{CH}_3$).²¹

4.1.3. (2E,6E)-1-Bromo-3,7,11-trimethyldodeca-2,6,10-triene (5)

To a solution of **4** (2.87 g, 12.9 mmol) in diethyl ether (15 mL) and pyridine (0.1 mL) under nitrogen atmosphere, PBr_3 (1.52 g, 5.6 mmol) in *n*-hexane (6 mL) was added slowly at 0 °C. The reaction mixture was stirred at 0 °C for 0.5 h and then was allowed to rise to the room temperature for 2 h. The upper layer was poured into ice water, and extracted with diethyl ether (20 mL \times 3). The organic layer was combined, washed with brine, dried over anhydrous Na_2SO_4 , and concentrated in vacuo to afford **5** as a colorless liquid (2.79 g, 76%).

4.1.4. Methyl thiosalicylate (7)

To a methanol solution (50 mL) of **6** (5.00 g, 32.5 mmol), SOCl_2 was added slowly and the mixture was stirred at 0 °C for 1 h. The obtained mixture was then heated to reflux for 6 h. The solvent was removed under reduced pressure. The residue was dissolved in ethyl acetate (50 mL), and washed with saturated NaHCO_3 (50 mL \times 2) and brine, dried with anhydrous Na_2SO_4 . The crude product was purified by silica gel chromatography (petroleum ether–ethyl acetate = 40:1 v/v as the eluent) to afford compound **7** as a colorless liquid (4.62 g, 85%).

4.1.5. Methyl 2-(((2E,6E)-3,7,11-trimethyldodeca-2,6,10-trien-1-yl)thio)benzoate (8)

A mixture of **7** (0.9 g, 6 mmol), K_2CO_3 (1.3 g, 7 mmol) and **3** (1.7 g, 6 mmol) in acetonitrile (75 mL) was refluxed for 6 h. The solvent was evaporated in vacuum and water was added. The solution was neutralized with 2 N HCl solution to pH 6–7, and then extracted with CH_2Cl_2 (20 mL \times 3). The organic layer was concentrated in vacuo and the residue was purified by column chromatography on silica gel (petroleum ether/ethyl acetate = 30:1, v/v as the eluent), yield **8** as a yellowish oil (1.83 g, 82%). ^1H NMR (CDCl_3 , 300 MHz, δ ppm): 7.92–7.96 (m, H, Ar-H), 7.69–7.74 (m, 1H, Ar-H), 7.26–7.30 (m, 1H, Ar-H), 7.11–7.14 (m, 1H, Ar-H), 5.34 (bt, 1H, SCH_2CH), 5.09 (bt, 2H, $2 \times \text{CH}_2\text{CH}=\text{CCH}_3$), 3.92 (s, 3H, OCH_3), 3.58 (d, 2H, $J = 7.8$ Hz, SCH_2), 1.89–2.02 (m, 8H, $2 \times \text{CCH}_2\text{CH}_2\text{CH}$), 1.50–1.68 (m, 12H, $4 \times \text{CH}=\text{CCH}_3$).²²

4.1.6. 2-(((2E,6E)-3,7,11-Trimethyldodeca-2,6,10-trien-1-yl)thio)benzoic acid (9)

To a solution of **5** (0.50 g, 1.34 mmol) in ethyl alcohol (25 mL), 1 N NaOH aqueous solution (2.5 mL) was added dropwise at the room temperature. The mixture was refluxed for 10 h, and then cooled. The solvent was evaporated and the residue was dissolved in 1 M HCl solution. The mixture was extracted with ethyl acetate (30 mL \times 3). The organic layer was combined, washed with brine, dried with anhydrous Na_2SO_4 and concentrated in vacuo, affording **9** as a pale yellow waxy solid (4.32 g, 90%). ^1H NMR (CDCl_3 , 300 MHz, δ ppm): 8.12–8.15 (m, H, Ar-H), 7.41–7.47 (m, 2H, Ar-H), 7.22–7.26 (m, 1H, Ar-H), 5.31 (bt, 1H, SCH_2CH), 5.09 (bt, 2H, $2 \times \text{CH}_2\text{CH}=\text{CCH}_3$), 3.57 (d, 2H, $J = 4.5$ Hz, SCH_2), 1.89–2.02 (m, 8H, $2 \times \text{CCH}_2\text{CH}_2\text{CH}$), 1.50–1.68 (m, 12H, $4 \times \text{CH}=\text{CCH}_3$); MS (ESI) $m/z = 357$ [$\text{M}-1$] $^+$; Anal. Calcd for $\text{C}_{22}\text{H}_{30}\text{O}_2\text{S}$: C, 73.70; H, 8.43. Found: C, 73.77; H, 8.84.¹⁸

4.1.7. General procedure for the preparation of 10a–g and 11a–g

The parent compound **9** (0.36 g, 1 mmol) was dissolved in CH_2Cl_2 (6 mL), then oxalyl chloride (4 mmol) was added dropwise. The mixture was stirred for 4 h at the room temperature. The solvent and excess oxalyl chloride was evaporated to obtain the crude farnesylthiosalicyl chloride. Then to a mixture of different diamines (1.5 mmol) and TEA (0.45 mmol) in 10 mL CH_2Cl_2 was added dropwise the CH_2Cl_2 solution (5 mL) of farnesylthiosalicyl chloride (1.12 g, 0.3 mmol) at 0 °C over 1 h. After stirring for another 0.5 h the reaction was quenched by adding 20 mL water. The mixture was extracted with CH_2Cl_2 (20 mL \times 3) and the organic layer was combined, washed with brine, dried with anhydrous Na_2SO_4 and concentrated in vacuo. The crude product was separated by silica gel chromatography (petroleum ether/ethyl acetate = 1:1 v/v; then CH_2Cl_2 –MeOH = 4:1 as the eluent) to afford compound **10a–g** and **11a–g** as yellowish oil.

4.1.8. *N*-(2-Aminoethyl)-2-(((2E,6E)-3,7,11-trimethyldodeca-2,6,10-trien-1-yl)thio)benzamide (10a)

Yellowish oil, 41.9% yield. IR (KBr, cm^{-1}): 3176, 1713, 1605, 1590, 1488; ^1H NMR (CDCl_3 , 300 MHz, δ ppm): 8.00 (br, 1H, NH), 7.75–7.78 (m, 1H, Ar-H), 7.32–7.37 (m, 2H, Ar-H), 7.18–7.20 (m, 1H, Ar-H), 5.23 (bt, 1H, SCH_2CH), 5.08 (bt, 2H, $2 \times \text{CH}_2\text{CH}=\text{CCH}_3$), 3.56 (d, 2H, $J = 9.0$ Hz, SCH_2), 2.99–3.05 (m, 4H, $2 \times \text{NCH}_2$), 1.91–2.05 (m, 8H, $2 \times \text{CCH}_2\text{CH}_2\text{CH}$), 1.53–1.68 (m, 12H, $4 \times \text{CH}_3$); ESI-MS (m/z): 401 [$\text{M}+\text{H}$] $^+$; Anal. Calcd for $\text{C}_{24}\text{H}_{36}\text{N}_2\text{O}_2\text{S}$: C, 71.95; H, 9.06; N, 6.99. Found: C, 71.86; H, 9.11; N, 7.01.

4.1.9. *N,N*-(Ethane-1,2-diyl)bis(2-(((2E,6E)-3,7,11-trimethyldodeca-2,6,10-trien-1-yl)thio)benzamide) (11a)

Yellowish oil, 36.2% yield. IR (KBr, cm^{-1}): 3132, 1708, 1611, 1583, 1471; ^1H NMR (CDCl_3 , 300 MHz, δ ppm): 7.65 (d, 2H, $J = 7.5$ Hz, Ar-H), 7.41–7.45 (m, 2H, Ar-H), 7.25–7.33 (m, 4H,

Ar-H), 6.86–6.89 (m, 2H, NH), 5.29–5.33 (m, 2H, SCH₂CH), 5.07–5.10 (m, 4H, CH₂CH=), 3.53–3.57 (d, 4H, *J* = 5.7 Hz, SCH₂), 3.19–3.23 (m, 4H, 2 × NCH₂), 1.96–2.00 (m, 16H, 4 × CCH₂CH₂CH), 1.53–1.63 (m, 24H, 8 × CH₃); MS (ESI) *m/z* = 742 [M+H]⁺; Anal. Calcd for C₄₆H₆₄N₂O₂S₂: C, 74.55; H, 8.70; N, 3.78. Found: C, 74.62; H, 8.61; N, 3.73.

4.1.10. *N*-(3-Aminopropyl)-2-(((2*E*,6*E*)-3,7,11-trimethyldodeca-2,6,10-trien-1-yl)thio)benzamide (10b)

Yellowish oil, 45.3% yield. IR (KBr, cm⁻¹): 3144, 1718, 1615, 1580, 1446; ¹H NMR (DMSO-*d*₆, 300 MHz, δ ppm): 7.79–7.93 (m, 2H, Ar-H), 7.26–7.32 (m, 2H, Ar-H), 5.21 (br, 1H, SCH₂CH), 5.12 (br, 2H, 2 × CH₂CH=), 3.51 (d, 2H, *J* = 9.0 Hz, SCH₂), 3.05 (m, 4H, 2 × NCH₂), 1.90–1.99 (m, 8H, 2 × CCH₂CH₂CH), 1.54–1.69 (m, 14H, 4 × CH₃, CH₂CH₂CH₂); ESI-MS (*m/z*): 415 [M+H]⁺; Anal. Calcd for C₂₅H₃₈N₂O₂S: C, 72.42; H, 9.24; N, 6.76. Found: C, 72.29; H, 9.18; N, 6.82.

4.1.11. *N,N'*-(Propane-1,3-diy)bis(2-(((2*E*,6*E*)-3,7,11-trimethyldodeca-2,6,10-trien-1-yl)thio)benzamide) (11b)

Yellowish oil, 31.5% yield. IR (KBr, cm⁻¹): 3206, 1720, 1619, 1583, 1458; ¹H NMR (CDCl₃, 300 MHz, δ ppm): 7.66–7.82 (m, 2H, Ar-H), 7.43–7.47 (m, 2H, Ar-H), 7.22–7.30 (m, 4H, Ar-H), 6.85–6.88 (m, 2H, NH), 5.30–5.33 (m, 2H, SCH₂CH), 5.08–5.12 (m, 4H, CH₂CH=), 3.53–3.57 (d, 4H, *J* = 9.0 Hz, SCH₂), 3.19–3.23 (m, 4H, 2 × NCH₂), 1.96–2.00 (m, 16H, 4 × CCH₂CH₂CH), 1.53–1.63 (m, 26H, 8 × CH₃, NCH₂CH₂); MS (ESI) *m/z* = 756 [M+H]⁺; Anal. Calcd for C₄₇H₆₆N₂O₂S₂: C, 74.75; H, 8.81; N, 3.71. Found: C, 74.78; H, 8.76; N, 3.85.

4.1.12. *N*-(4-Aminobutyl)-2-(((2*E*,6*E*)-3,7,11-trimethyldodeca-2,6,10-trien-1-yl)thio)benzamide (10c)

Yellowish oil, 46.9% yield. IR (KBr, cm⁻¹): 3184, 1715, 1610, 1578, 1457; ¹H NMR (DMSO-*d*₆, 300 MHz, δ ppm): 8.19 (br, 1H, NH), 7.78–7.84 (m, 1H, Ar-H), 7.36–7.41 (m, 2H, Ar-H), 7.20–7.23 (m, 1H, Ar-H), 5.23 (bt, 1H, SCH₂CH), 5.07 (bt, 2H, 2 × C=CH), 3.55 (d, 2H, *J* = 9.0 Hz, SCH₂), 3.12–3.27 (m, 4H, 2 × NCH₂), 1.91–2.03 (m, 8H, 2 × CCH₂CH₂CH), 1.53–1.64 (m, 12H, 4 × CH₃, 2 × NCH₂CH₂); ESI-MS (*m/z*): 429 [M+H]⁺; Anal. Calcd for C₂₆H₄₀N₂O₂S: C, 72.85; H, 9.41; N, 6.53. Found: C, 72.79; H, 9.42; N, 6.63.

4.1.13. *N,N'*-(Butane-1,4-diy)bis(2-(((2*E*,6*E*)-3,7,11-trimethyldodeca-2,6,10-trien-1-yl)thio)benzamide) (11c)

Yellowish oil, 33.0% yield. IR (KBr, cm⁻¹): 3145, 1716, 1612, 1580, 1460; ¹H NMR (CDCl₃, 300 MHz, δ ppm): 7.66 (d, 2H, *J* = 7.5 Hz, Ar-H), 7.40–7.45 (m, 2H, Ar-H), 7.23–7.36 (m, 4H, Ar-H), 6.88–6.93 (br, 2H, NH), 5.23–5.27 (d, 2H, *J* = 5.7 Hz, 2 × SCH₂CH), 5.03–5.08 (m, 4H, 4 × C=CH), 3.53–3.52 (m, 8H, 2 × SCH₂, 2 × NCH₂), 1.97–2.01 (m, 16H, 4 × CCH₂CH₂CH), 1.50–1.77 (m, 28H, 8 × CH₃, 2 × NCH₂CH₂); MS (ESI) *m/z* = 770 [M+H]⁺; Anal. Calcd for C₄₈H₆₈N₂O₂S₂: C, 74.95; H, 8.91; N, 3.64. Found: C, 75.10; H, 8.87; N, 3.52.

4.1.14. *N*-(5-Aminopentyl)-2-(((2*E*,6*E*)-3,7,11-trimethyldodeca-2,6,10-trien-1-yl)thio)benzamide (10d)

Yellowish oil, 48.1% yield. IR (KBr, cm⁻¹): 3181, 1716, 1611, 1582, 1461; ¹H NMR (DMSO-*d*₆, 300 MHz, δ ppm): 8.18 (br, 1H, NH), 7.78–7.83 (m, 1H, Ar-H), 7.35–7.42 (m, 2H, Ar-H), 7.18–7.22 (m, 1H, Ar-H), 5.23 (bt, 1H, SCH₂CH), 5.02–5.03 (m, 2H, 2 × C=CH), 3.56 (d, 2H, *J* = 9.0 Hz, SCH₂), 3.17–3.33 (m, 4H, 2 × NCH₂), 1.92–2.06 (m, 8H, 2 × CCH₂CH₂CH), 1.49–1.63 (m, 16H, 4 × CH₃, 2 × NCH₂CH₂), 1.31–1.35 (m, 2H, NCH₂CH₂CH₂); ESI-MS (*m/z*): 443 [M+H]⁺; Anal. Calcd for C₂₇H₄₂N₂O₂S: C, 73.25; H, 9.56; N, 6.33. Found: C, 73.12; H, 9.61; N, 6.48.

4.1.15. *N,N'*-(Pentane-1,5-diy)bis(2-(((2*E*,6*E*)-3,7,11-trimethyldodeca-2,6,10-trien-1-yl)thio)benzamide) (11d)

Yellowish oil, 30.4% yield. IR (KBr, cm⁻¹): 3127, 1710, 1603, 1574, 1448; ¹H NMR (CDCl₃, 300 MHz, δ ppm): 7.68 (d, 2H, *J* = 7.5 Hz, Ar-H), 7.41–7.43 (m, 2H, Ar-H), 7.21–7.33 (m, 2H, Ar-H), 6.86–6.87 (m, 2H, NH), 5.24–5.27 (m, 2H, 2 × SCH₂CH), 5.03~5.07 (m, 4H, 4 × C=CH), 3.49–3.52 (m, 8H, 2 × SCH₂, 2 × NCH₂), 1.95–2.04 (m, 16H, 4 × CCH₂CH₂CH), 1.39–1.71 (m, 30H, 8 × CH=CCH₃, 2 × NCH₂CH₂, NCH₂CH₂CH₂); MS (ESI) *m/z* = 784 [M+1]⁺; Anal. Calcd for C₄₉H₇₀N₂O₂S₂: C, 75.14; H, 9.01; N, 3.58. Found: C, 75.23; H, 9.12; N, 3.46.

4.1.16. *N*-(6-Aminoethyl)-2-(((2*E*,6*E*)-3,7,11-trimethyldodeca-2,6,10-trien-1-yl)thio)benzamide (10e)

Yellowish oil, 60.2% yield. IR (KBr, cm⁻¹): 3184, 1723, 1625, 1588, 1468; ¹H NMR (DMSO-*d*₆, 300 MHz, δ ppm): 8.20 (br, 1H, NH), 7.75–7.81 (m, 1H, Ar-H), 7.30–7.36 (m, 2H, Ar-H), 7.20 (m, 1H, Ar-H), 5.22 (bt, 1H, SCH₂CH), 5.06 (bt, 2H, 2 × C=CH), 3.55 (d, 2H, *J* = 9.0 Hz, SCH₂), 3.15–3.21 (m, 4H, 2 × NCH₂), 1.95–2.05 (m, 8H, 2 × CCH₂CH₂CH), 1.47–1.63 (m, 16H, 2 × NCH₂CH₂, 4 × CH₃), 1.31–1.36 (m, 2H, NCH₂CH₂CH₂); ESI-MS (*m/z*): 457 [M+H]⁺; Anal. Calcd for C₂₈H₄₄N₂O₂S: C, 73.63; H, 9.71; N, 6.13. Found: C, 73.48; H, 9.76; N, 6.25.

4.1.17. *N,N'*-(Hexane-1,6-diy)bis(2-(((2*E*,6*E*)-3,7,11-trimethyldodeca-2,6,10-trien-1-yl)thio)benzamide) (11e)

Yellowish oil, 25.8% yield. IR (KBr, cm⁻¹): 3166, 1708, 1603, 1576, 1452; ¹H NMR (CDCl₃, 300 MHz, δ ppm): 7.67 (d, 2H, *J* = 7.5 Hz, Ar-H), 7.41–7.47 (m, 2H, Ar-H), 7.24–7.33 (m, 4H, Ar-H), 6.86–6.87 (br, 2H, NH), 5.24–5.27 (m, 2H, 2 × SCH₂CH), 5.04–5.09 (m, 4H, 4 × C=CH), 3.45–3.54 (m, 8H, 2 × SCH₂, 2 × NCH₂), 1.95–2.09 (m, 16H, 4 × CCH₂CH₂CH), 1.48–1.70 (m, 32H, 8 × CH₃, 2 × NCH₂CH₂, 2 × NCH₂CH₂CH₂); MS (ESI) *m/z* = 798 [M+1]⁺; Anal. Calcd for C₅₀H₇₂N₂O₂S₂: C, 75.33; H, 9.10; N, 3.51. Found: C, 75.42; H, 9.06; N, 3.39.

4.1.18. *N*-(2-(2-Aminoethoxy)ethyl)-2-(((2*E*,6*E*)-3,7,11-trimethyldodeca-2,6,10-trien-1-yl)thio)benzamide (10f)

Yellowish oil, 52.6% yield. IR (KBr, cm⁻¹): 3181, 1719, 1616, 1585, 1466; ¹H NMR (DMSO-*d*₆, 300 MHz, δ ppm): 8.18 (br, 1H, NH), 7.41–7.46 (m, 3H, Ar-H), 7.22–7.26 (m, 1H, Ar-H), 5.28–5.32 (m, 1H, SCH₂CH), 5.07–5.09 (m, 2H, 2 × CH₂CH=CCH₃), 3.49–3.82 (m, 10H, SCH₂, 2 × NCH₂CH₂O), 1.91–2.01 (m, 8H, 2 × CCH₂CH₂CH), 1.53–1.68 (m, 12H, 4 × CH₃); MS (ESI) *m/z* = 445 [M+1]⁺; Anal. Calcd for C₂₆H₄₀N₂O₂S: C, 70.23; H, 9.07; N, 6.30. Found: C, 70.17; H, 9.01; N, 6.35.

4.1.19. *N,N'*-(Oxybis(ethane-2,1-diy)bis(2-(((2*E*,6*E*)-3,7,11-trimethyldodeca-2,6,10-trien-1-yl)thio)benzamide) (11f)

Yellowish oil, 29.2% yield. IR (KBr, cm⁻¹): 3169, 1717, 1618, 1581, 1463; ¹H NMR (CDCl₃, 300 MHz, δ ppm): 7.68–7.72 (m, 2H, Ar-H), 7.42–7.76 (m, 2H, Ar-H), 7.23–7.32 (m, 2H, Ar-H), 6.65–6.68 (br, 2H, NH), 5.31 (m, 2H, 2 × SCH₂CH), 5.08 (m, 4H, 4 × CH₂CH=CCH₃), 3.47–3.79 (m, 12H, 2 × SCH₂, 2 × NCH₂CH₂O), 1.89–2.03 (m, 16H, 4 × CCH₂CH₂CH), 1.53–1.69 (m, 24H, 8 × CH₃); MS (ESI) *m/z* = 786 [M+1]⁺; Anal. Calcd for C₄₈H₆₈N₂O₃S₂: C, 73.42; H, 8.73; N, 3.57. Found: C, 73.56; H, 8.82; N, 3.43.

4.1.20. Piperazin-1-yl(2-(((2*E*,6*E*)-3,7,11-trimethyldodeca-2,6,10-trien-1-yl)thio)phenyl)methanone (10g)

Yellowish oil, 44.7% yield. IR (KBr, cm⁻¹): 3170, 1715, 1608, 1581, 1461; ¹H NMR (DMSO-*d*₆, 300 MHz, δ ppm): 7.41–7.47 (m, 3H, Ar-H), 7.23–7.26 (m, 1H, Ar-H), 5.31 (bt, 1H, SCH₂CH), 5.09 (bt, 2H, 2 × CH₂CH=CCH₃), 3.57 (d, 2H, *J* = 4.5 Hz, SCH₂), 3.06–3.23 (m, 8H, 4 × NCH₂), 1.89–2.02 (m, 8H, 2 × CCH₂CH₂CH), 1.50–1.68 (m, 12H, 4 × CH₃); MS (ESI) *m/z* = 427 [M+1]⁺; Anal.

Calcd for C₂₆H₃₈N₂O₂S: C, 73.19; H, 8.98; N, 6.57. Found: C, 73.03; H, 8.91; N, 6.74.

4.1.21. Piperazine-1,4-diylbis(2-(((2E,6E)-3,7,11-trimethyldodeca-2,6,10-trien-1-yl)thio)phenyl)methanone (11g)

Yellowish oil, 36.2% yield. IR (KBr, cm⁻¹): 3147, 1708, 1606, 1583, 1459; ¹H NMR (CDCl₃, 300 MHz, δ ppm): 7.42–7.57 (m, 4H, Ar-H), 7.32–7.39 (m, 2H, Ar-H), 7.17–7.21 (m, 2H, Ar-H), 5.31 (bt, 2H, 2 × SCH₂CH), 5.04–5.09 (m, 2H, 4 × CH₂CH=), 3.57 (d, 4H, J = 4.5 Hz, 2 × SCH₂), 3.12–3.21 (m, 8H, NCH₂), 1.89–2.02 (m, 16H, 4 × CCH₂CH₂CH), 1.50–1.68 (m, 24H, 8 × CH₃); MS (ESI) m/z = 768 [M+1]⁺; Anal. Calcd for C₄₈H₆₆N₂O₂S₂: C, 75.15; H, 8.67; N, 3.65. Found: C, 75.32; H, 8.76; N, 3.49.

4.2. Biological evaluation

4.2.1. MTT assay

SGC7901 (human gastric cancer cells), SMMC-7721 (human hepatocellular carcinoma cells), EJ (human bladder carcinoma cells), SKOV-3 (human ovarian cancer cells), MCF-7 (human breast cancer cells), H460 (human lung cancer cells), or Panc-1 (human pancreatic carcinoma cells) at 10⁴ cells per well were cultured in 10% FBS DMEM in 96-well flat-bottom microplates overnight. The cells were incubated in triplicate with, or without, different concentrations of each test compound for 48 h. During the last 4 h incubation, 30 μL of tetrazolium dye (MTT) solution (5 mg mL⁻¹) was added to each well. The resulting MTT-formazan crystals were dissolved in 150 μL DMSO, and absorbance was measured spectrophotometrically at 570 nm using an ELISA plate reader. The inhibition induced by each test compound at the indicated concentrations was expressed as a percentage. The concentration required for 50% inhibition (IC₅₀) was calculated using the software (GraphPadPrism Version 4.03).

4.2.2. Flow cytometry assay of cell apoptosis

SMMC-7721 cells were cultured overnight and incubated in triplicate with the test compound (3.0, 6.0 and 12 μmol/L) or vehicle for 48 h. The cells were harvested, and stained with FITC-Annexin V and PI (BioVision) at room temperature for 15 min. The percentage of apoptotic cells was determined by flow cytometry (Beckman Coulter) analysis.

4.2.3. Western blot assay

The mechanisms of the cell apoptosis and the inhibitory activity of Ras-related signaling were determined by western blot assay. SMMC-7721 cells at 1.5 × 10⁵/mL were treated with 3.0, 6.0 or 12 μmol/L **10f** or vehicle control for 8 h. After harvested and lysed, the cell lysates (50 μg/lane) were separated by SDS-PAGE (12% gel) and transferred onto nitrocellulose membranes. After blocked with 5% fat-free milk, the target proteins were probed with anti-Bcl-2, anti-Bax, anti-caspase-3, anti-Akt, anti-phospho-Akt (Ser473), anti-ERK, anti-phospho-ERK (Thr202/Tyr204), and anti-β-actin antibodies (Cell Signaling, Boston), respectively. The bound antibodies were detected by HRP-conjugated second antibodies and visualized using the enhanced chemiluminescent reagent. The

relative levels of each signaling event to control β-actin were determined by densitometric scanning.

4.3. Aqueous solubility

Each test compound (about 20.0 mg) was placed in a 25 mL ground flask. Then 5 mL 10% PEG400 water solution was added and exposed to ultrasonic oscillation for 10 min. The mixture was allowed to stir for 24 h in a water bath at 25 °C. The obtained water suspension solution was centrifuged for 10 min (10,000 rpm), and the clear supernatant was filtered out through a microporous membrane and injected to the HPLC system for concentration determination using a standard curve.

Acknowledgments

We gratefully acknowledge the financial support by the Natural Science Foundation of China (Grant Nos. 81302628 and 81202467) and Jiangsu Province (Grant Nos. BK2011389 and BK2012232), the Natural Science Research Project of Universities in Jiangsu Province of China (11KJB350004), Applied Research Projects of Nantong City (BK2012085), and also thank a project funded by the Priority Academic Programs Development of Jiangsu Higher Education Institutions (PAPD).

References and notes

- Maity, A.; Pore, N.; Lee, J.; Solomon, D.; O'Rourke, D. M. *Cancer Res.* **2000**, *60*, 5879.
- Porfiri, E.; McCormick, F. J. *Biol. Chem.* **1996**, *271*, 5871.
- Adjei, A. A. J. *Natl. Cancer Inst.* **2001**, *93*, 1062.
- Karnoub, A. E.; Weinberg, R. A. *Nat. Rev. Mol. Cell Biol.* **2008**, *9*, 517.
- Downward, J. *Nat. Rev. Cancer* **2003**, *3*, 11.
- Chin, L.; Tam, A.; Pomerantz, J.; Wong, M.; Holash, J.; Bardeesy, N.; Shen, Q.; O'Hagan, R.; Pantginis, J.; Zhou, H.; Horner, J. W., 2nd; Cordon-Cardo, C.; Yancopoulos, G. D.; DePinho, R. A. *Nature* **1999**, *400*, 468.
- Haklai, R.; Weisz, M. G.; Elad, G.; Paz, A.; Marciano, D.; Egozi, Y.; Ben-Baruch, G.; Kloog, Y. *Biochemistry* **1998**, *37*, 1306.
- Marom, M.; Haklai, R.; Ben-Baruch, G.; Marciano, D.; Egozi, Y.; Kloog, Y. *J. Biol. Chem.* **1995**, *270*, 22263.
- Elad, G.; Paz, A.; Haklai, R.; Marciano, D.; Cox, A.; Kloog, Y. *Biochim. Biophys. Acta* **1999**, *1452*, 228.
- Haklai, R.; Elad-Sfadia, G.; Egozi, Y.; Kloog, Y. *Cancer Chemother. Pharmacol.* **2008**, *61*, 89.
- Tsimberidou, A. M.; Rudek, M. A.; Hong, D.; Ng, C. S.; Blair, J.; Goldsweig, H.; Kurzrock, R. *Cancer Chemother. Pharmacol.* **2009**, *65*, 235.
- Zundeleovich, A.; Elad-Sfadia, G.; Haklai, R.; Kloog, Y. *Mol. Cancer Ther.* **2007**, *6*, 1765.
- Bustanza-Linares, E.; Kurzrock, R.; Tsimberidou, A. M. *Future Oncol.* **2010**, *6*, 885.
- Biran, A.; Brownstein, M.; Haklai, R.; Kloog, Y. *Int. J. Cancer* **2012**, *128*, 691.
- Ling, Y.; Ye, X.; Zhang, Z.; Zhang, Y.; Lai, Y.; Ji, H.; Peng, S.; Tian, J. J. *Med. Chem.* **2011**, *54*, 3251.
- Cogoi, S.; Shchekotikhin, A. E.; Membrino, A.; Sinkevich, Y. B.; Xodo, L. E. *J. Med. Chem.* **2013**, *56*, 2764.
- St. Jean, D. J., Jr.; Fotsch, C. J. *Med. Chem.* **2012**, *55*, 6002.
- Marciano, D.; Ben-Baruch, G.; Marom, M.; Egozi, Y.; Haklai, R.; Kloog, Y. *J. Med. Chem.* **1995**, *38*, 1267.
- Thulasiram, H. V.; Poulter, C. D. J. *Am. Chem. Soc.* **2006**, *128*, 15819.
- Hess, S.; Akermann, M. A.; Wnendt, S.; Zwingenberger, K.; Eger, K. *Bioorg. Med. Chem.* **2001**, *9*, 1279.
- Gibbs, R. A.; Krishnan, U.; Dolence, J. M.; Poulter, C. D. J. *Org. Chem.* **1995**, *60*, 7821.
- Kloog, Y.; Brownstein, M.; Chapman, J.; Karussis, D.; Bruck, R.; Reif, S. *WO 2000078303*, **2000**.